Julian Zobel, Patrick Lieser, Bastian Drescher, Bernd Freisleben and Ralf Steinmetz. *Optimizing Inter-Cluster Flights of Post-Disaster Communication Support UAVs*. Accepted for publication in Proc. of the 44th IEEE Conference on Local Computer Networks (LCN), 2019.

Optimizing Inter-Cluster Flights of Post-Disaster Communication Support UAVs

Julian Zobel*‡, Patrick Lieser*, Bastian Drescher*, Bernd Freisleben†, Ralf Steinmetz*
*Technische Universität Darmstadt, Germany
†Philipps-Universität Marburg, Germany
‡E-Mail: julian.zobel@kom.tu-darmstadt.de

***Abstract*—In the aftermath of large-scale disasters, critical communication infrastructure is often destroyed. Ad hoc networks can restore wireless communication with basic functionalities, especially for civilians in the affected areas. However, as humans form groups and tend to stay around important locations like shelters in such situations, the network is highly intermittent. Autonomous Unmanned Aerial Vehicles can act as controllable and highly mobile data carriers between separated network clusters to enable delay-tolerant inter-cluster communication. A possible heterogeneous set of usable aerial vehicles and the necessity to adapt the system to various environments requires the system to be highly flexible. Combined with severe constraints in energy usage or number of available vehicles, there is a need to increase the efficiency of inter-cluster flights. In this paper, we present approaches to optimize inter-cluster flights based on communication performance and energy efficiency. The resulting optimization model is a powerful tool for operators to adjust system settings to match required demands.**

I. Introduction

The number of natural large-scale extreme weather disasters such as floods and hurricanes has risen significantly in recent years and is expected to further increase in the future [22]. In the aftermath of such events, critical infrastructure for information and communication technologies (ICT) is often destroyed [15], [30], although functioning ICT has shown to be an important factor in reducing disaster-related fatalities [22]. Device-to-device communication among smart mobile devices and the formation of large, delay-tolerant mobile ad hoc networks (DTN-MANET) within the affected areas can relief the situation especially for civilians, by providing basic communication functionalities [2], [10], [11]. However, humans have shown to naturally form groups and to stay around important locations such as shelters and power or water resources in disaster situations. This severely limits the communication performance in the disaster area, as the network is highly intermittent and mobility between distinct network clusters is rare [2], [10].

To establish inter-cluster communication, message relaying over mobile data carriers is an effective technique [27], [28]. Especially in disaster scenarios, Unmanned Aerial Vehicles (UAVs) have several advantages over both static and ground-based relays. As a UAV system can be deployed where and whenever it is needed, it is highly flexible and allows for a quick and situation-adapted deployment. Furthermore, aerial vehicles are independent of flooded, obstructed, or destroyed roads and can move in a direct line between points-of-interest, rendering them highly mobile in contrast to pedestrians or cars. Besides, sensing capabilities of UAVs provide valuable information for operators or the system to detect temporary or unexpected events, which require the system to adapt [27]. We have shown the applicability of autonomous UAVs and their impact on intermittent DTN-MANETs in previous work [13], with the focus on small, autonomous commodity multicopter UAVs due to wide availability, low costs, pilot-less flight, and in particular their ability to hover. Simulations suggest that a communication support system comprised of just a few UAVs significantly decreases the delay until messages arrive and also increases the message spread throughout the intermittent network. However, communication performance of the inter-cluster links is strongly dependent on factors such as the present disaster scenario and the DTN-MANET, but also on the available UAVs, their flight properties, battery capacity, or similar, which was not considered up to this point.

To provide optimal performance in regard to different objectives like fast data delivery in the network or low power consumption on the UAVs, operators of the aerial communication support system have to consider a plethora of parameters. As, e.g., the set of available UAVs can be highly heterogeneous with different ranges, velocities, flight times, and more, taking only a few parameters into account for an suitable solution is very complex. Furthermore, the requirements on the support system can change constantly due to temporary or unexpected events, and thus, parameters must be re-evaluated and the system must be adapted to the new situation, which poses an additional burden for operating personnel. In this paper we therefore present three approaches to optimize inter-cluster flights based on distinct system demands and highlight their differences. An existing simulation framework [13] was enhanced with a configurable optimization model, that is able to combine different optimization objectives. This model gives system operators the ability to analyze communication as well as system performance under various settings, and eventually to find the optimal system settings to match the demanded requirements. The existing framework did only provide a static power consumption model for hovering and full speed flight, which is not suitable to model power consumption of UAVs realistically. Thus, we also integrated a velocity-based energy consumption model for multicopter propulsion based

on specifications and measurements of a real-world UAV that allows a more realistic energy consumption estimation of the UAV system.

The paper is structured as follows. Initially, we present related work for inter-cluster communication and trajectory optimization of data ferry UAVs in Section II. Our energy consumption model is presented in Section III. Afterwards, Section IV describes different objectives for optimizing data ferry links and the combined optimization model, which is then evaluated in Section V. Section VI concludes the paper.

II. Related Work

Overcoming partitions in a Mobile Ad Hoc Network (MANET) and transferring messages between intermittent network clusters is generally approached by adding disruption- and delay-tolerance to the communication protocols [1], [17], [24]. In the resulting delay-tolerant ad hoc networks (DTN-MANETs), every node can act as a mobile relay, thus, carrying received messages around and distributing them when connecting with other nodes. More sophisticated protocols [9], [14], [21], [25] use group formations or encounter probabilities to mitigate common problems like broadcast storms or overfilled data memories. However, node mobility is required for a working communication, but is especially in a post-disaster scenario very slow or even impossible due to obstructed and destroyed roads or the common human trait of group formation and highly static clustering around important locations such as shelters [2]. Introducing specialized and usually controllable mobile relay nodes, also called message or data ferries, has shown to greatly improve the communication in intermittent networks [23], [28], [29].

With the increasing availability and falling costs for Unmanned Aerial Vehicles (UAV), either fixed-wing planes or rotary-wing multicopters, they have gained significant attention for their applicability as highly mobile and controllable data relays or data collectors. Connecting multiple locations by an optimal route, known as either the Minimum Latency Problem [4] or the Travelling Salesman Problem [5], is an np-hard calculation, and thus, most often heuristics and algorithms are used to calculate optimal trajectories [7], [28]. In [28], a simple nearest neighbor heuristic is compared with a traffic-aware algorithm, which takes the number of messages and the location of their destination in consideration, to improve connectivity in the network. Similarly, gradient-based trajectory algorithms for optimal connectivity of ground nodes are proposed in [7]. Besides general connectivity, trajectories can be optimized to allow for maximized data throughput or to minimize required transmission power for data exchange in the network [29]. An increase in data throughput with decreased transmission power by optimizing a UAV's trajectory is achieved in [27]. Mozaffari et al. [16] used UAVs to collect data of multiple static IoT devices to decrease transmission energy of the devices used for long-range communication to a central data sink. Pearre et al. [19] used reinforced learning and stochastic techniques to optimize UAV trajectories to allow distributed sensors in a wide-spread network to minimize its transmission power similarly. To connect distinct emergency shelters with large data loads and considerable up- and downlink times with the Internet, a genetic algorithm is used in [3].

For a fixed-wing UAV, power-efficient trajectories towards an objective based on the UAV's constraints in movement and power consumption are calculated in [26]. A theoretical energy consumption model for a multicopter UAV is provided in [16]. In contrast to these two examples, either for fixed-wing or multicopter UAVs, most approaches assume the deployed UAVs to be generally appropriate for the scenario and do not take power consumption of UAVs into account. However, in our case of long-term inter-cluster communication provision with small commodity hardware, power consumption of the UAV has a significant influence on the system performance and runtime. It is therefore necessary to have a realistic energy model for the used UAVs to obtain meaningful results.

III. Propulsion Energy Consumption Model

The simulation framework we presented in previous work [13] used a simple movement and energy model, which consumed energy at a constant rate for flying and for hovering. Adjusting the speed did not influence the amount of consumed energy. To enable a more realistic evaluation of different speeds and their impact on flight duration and performance, we created a sophisticated energy consumption model for multicopter UAV propulsion. This model is based on available specifications and conducted lab measurements with the *Intel Aero Ready-to-Fly Drone*[1].

Initially, we reviewed the officially available specifications and measured the energy requirements of the UAV. The manufacturer's specification state that the UAV is able to hover for 20 to 24 minutes with a 4000 mAh 4S LiPo battery. In that case, the power draw of each of the rotors would be between 2.5 A and 3 A at the given supply voltage of 14.8 V. We made an indoor flight test with a slightly smaller and lighter 3700 mAh 4S LiPo battery for full 22 minutes, after which the battery was at 15% charge. The overall power draw was around 8.6 A, however, this also includes power consumption from the onboard computer, which is specified to 10 W, and maneuvers that were necessary to hold the UAV steady. Furthermore, we note that the indoor lab measurements did neither include wind nor movement from the UAV, and thus, power consumption in realistic environments will most likely be higher.

In the next step, we assessed the thrust provided by the four 9x6 inches two-bladed propellers. The University of Illinois at Urbana-Champaign provides a database of propeller performance data [6], which we used to reconstruct the performance of the Aero Drone. Since there are no official specifications on the used propellers, we used the performance data of a comparable 9x6 inches APC propeller.

The provided thrust $T(n)$ of a propeller is calculated by

$$T(n) = c_{T,n}\ \rho\ n^2\ D^4 \tag{1}$$

[1]Specifications for the Intel Aero Ready to Fly Drone: https://www.intel.com/content/www/us/en/support/articles/000023272/drones/development-drones.html (accessed 01.08.2019)

where n is the number of revolutions per second, $c_{T,n}$ is the thrust coefficient of the propeller at the given n, ρ is the air density, and D is the propeller diameter [18]. For simplification, we chose $\rho = 1.2045 \frac{kg}{m^3}$ statically, which is the air density at $20°C$ and a height of 30 meters. The diameter of the propeller is 22.86 cm (9 inches). The weight of the UAV including the 3700 mAh LiPo battery is 1.237 kg, and thus, an upward force F_H = 12.131 N is required for the UAV to hover, or around 3 N from each rotor. In the performance data we found that approximately 5000 RPM are required by such a propeller to provide this force. With the given value of $c_{T,5000}$ [6] we use Equation 1 to calculate n as

$$n = \sqrt{\frac{T(n)}{c_{T,n}\ \rho\ D^4}} \tag{2}$$

which gives us 5005 RPM as the specific value necessary for hovering the UAV. Furthermore, we use the propeller power equation in [20]

$$P(n) = c_{P,n}\ \rho\ n^3\ D^5 \tag{3}$$

together with $c_{P,5000}$ from the database to calculate that 1.86 A would be required to drive each propeller, or 7.44 A in total. In comparison with the values obtained from the indoor flight test, the calculated values show a high correlation. The additional 1.1 A in the indoor flight test can, as already stated, be attributed to the onboard computer and required maneuvers.

The performance data shows a high usability to calculate realistic values for the provided thrust and the required power. For the simulations, we wanted to enhance the UAV performance, and thus, increased the battery capacity to a realistic maximum. With the available maximum thrust $T(8200\frac{1}{s}) = 7.4\ N$ per rotor and 865 g dry mass of the UAV, around 660 g of battery can be added such that the thrust-weight-ratio stays above 2.0, which is necessary for the UAV to maintain highly maneuverable. A 6600 mAh battery has shown to be the largest size fitting on the UAV without increasing the overall takeoff weight too much, and is, therefore, used in the simulations. Nevertheless, the proposed model is flexible and can handle an arbitrary battery size.

We calculated several key performance characteristics, that will later on allow the stateless calculation of thrust and current with the propulsion energy consumption model. This includes the minimum and maximum motor speeds (2500 RPM and 8200 RPM[2]), the thrust required for a safe vertical descent and ascent velocity of $5\frac{m}{s}$, respectively, and hovering. Thrust calculations for specific velocities can be approximated using the air drag [18], [26] on the UAV as

$$D(v) = \frac{1}{2}\ \rho\ v^2\ A\ c_D \tag{4}$$

on the one hand, and the thrust required to keep the velocity v stable (Eq. 1) on the other hand, where A is the area exposed to drag, in this case the top or bottom area, respectively, and the drag coefficient c_D of the UAV. Eventually, seven motor characteristics are used for the propulsion energy consumption model in the simulation, which are stated in Table I, consisting of provided thrust and required current draw.

[2]Intel Aero RTF Drone: Intel Forum Entry on Motor Specifications, https://forums.intel.com/s/question/0D50P0000490HoiSAE/request-for-motor-esc-and-propeller-specs (accessed 01.08.2019)

TABLE I: Motor characteristics used in the simulator. Values are stated per each rotor.

RPM	c_T	c_P	Thrust [N]	Current [A]	Note
2500	0.1291	0.0610	0.74	0.22	Idle state
4000	0.1245	0.0652	1.82	0.98	
5150	0.1263	0.0648	3.06	2.08	$5\frac{m}{s}$ descent
5550	0.1293	0.0630	3.60	2.53	Hover
6000	0.1273	0.0640	4.19	3.25	$5\frac{m}{s}$ ascent
7000	0.1232	0.0649	5.52	5.24	
8200	0.1210	0.0647	7.43	8.39	Full throttle

TABLE II: Total thrust F_T, induced forward thrust F_v, and theoretically achievable horizontal velocity v_h with respect to a specific pitch angle α.

α	F_T [N]	F_v [N]	$v_h[\frac{m}{s}]$
5°	14.46	1.26	5
10°	14.62	2.54	6.5
20°	15.32	5.24	8.3
45°	20.36	14.4	12
60°	28.80	23.94	15.7

The simulator looks up the thrust that is required to reach or hold a specific velocity, and receives the corresponding current. Values which are not directly provided by a characteristic are interpolated between the next lower and next higher characteristics. The amount of thrust required for a specific velocity v can be—similarly to the vertical movement—calculated by finding the thrust F_v in movement direction that is equal to the induced drag D_v (Eq. 4). In case of pure horizontal movement, F_v can be easily deduced from the thrust F_H required to hold the altitude and the forward pitch angle α:

$$F_v = \tan(\alpha) F_H. \tag{5}$$

Clearly, as α increases, F_H also has to increase to hold the altitude steady. The increase for small angles, however, is very small. The forward thrust induced on the UAV also induces air drag, that ultimately defines how fast the UAV can move in the equilibrium of forces. The maximum possible horizontal velocity at a given pitch angle α and a given forward thrust F_v can be calculated as

$$v(\alpha) = \sqrt{\frac{2F_v}{\rho A_\alpha c_D}} = \sqrt{\frac{2\tan(\alpha)F_H}{\rho A_\alpha c_D}}. \tag{6}$$

By pitching the aircraft, the size of the exposed area in the forward direction is also changing, and thus, A_α has to be calculated as

$$A_\alpha = \sin(\alpha) A_{top/bottom} + \cos(\alpha) A_{front/rear} \tag{7}$$

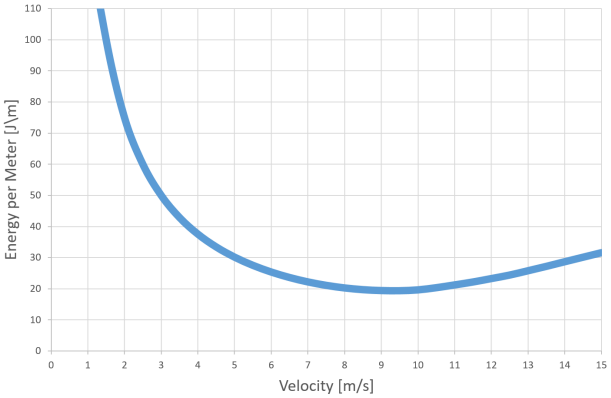

Fig. 1: Required energy to move the UAV a meter for a certain velocity. The minimum refers to the most efficient flight velocity, that is 9 $\frac{m}{s}$ in case of our real-world UAV.

with the simplification of equal areas for the top and bottom as well as the front and rear faces, respectively. Interestingly, due to the quadratic increase of air drag and the relatively small front facing area, low pitch angles yield already comparably large horizontal velocities. Similarly, the overall increase in pitch angle and induced forward thrust lets the velocity grow asymptotically towards the maximum [18]. As an example, pitching the UAV to $\alpha = 5°$ will give a maximum possible horizontal velocity of $v_{\alpha=5°} = 5\frac{m}{s}$ using Equation 6. Counter-intuitively, this only requires an approximated 9% increase in overall thrust, but is compliant to flight tests with the drone, where low pitch angles resulted in unexpected high speeds. However, a small α will lead to low acceleration, and thus, the UAV most likely will accelerate with higher pitch angle and thrust first but then pitch and throttle back to hold the desired velocity with the most efficient setting. More examples for pitch angles α and their respective maximum horizontal velocities v_h are found in Table II. The relation between energy consumption and flown distance is shown in Figure 1.

With this new model for a multicopter's propulsive energy consumption, it is now possible to assess the system's efficiency based on different velocities and respective power consumption. Up to this point, we do not incorporate additional influences such as wind or the change of air density in relation to height or temperature.

IV. Optimizing Data Ferry Links

We applied autonomous UAVs on highly intermittent DTN-MANETs in previous work [13] and have shown their significant impact on the overall communication performance. Due to wide availability, low costs, pilot-less flight, and the ability to hover, which grants more stable communication links than during movement [8], we solely focus on small and autonomously flying commodity multicopter UAVs. They, however, have severe restrictions especially regarding flight times in contrast to larger multicopter or fixed-wing UAVs in general. As simulations have shown, an increase in the number of deployed UAVs using data ferries among all network clusters [3], [28] does not necessarily increase the communication performance, due to the transport routes of data ferries getting saturated quickly [13]. It is therefore more efficient, especially in large-scale scenarios where routes may be too long for the UAVs to complete them, to establish 1-to-1 connections between network clusters instead of routing UAVs over all of them. On these data ferry links, UAVs directly oscillate between clusters, and thus, data is distributed more evenly and more quickly than in the former case. Although not part of this work, we note that data ferry links connecting multiple network clusters can be found, for example, by calculating a minimum spanning tree over all clusters using Prim's or Kruskal's algorithm.

Through the course of a disaster, the requirements on the overall communication and the type and amount of data that is being distributed can change dramatically [12]. For example, emergency calls need to be distributed very fast and reliable to allow quick responses of emergency services or voluntary helpers, whereas private messages between friends and families should be delivered within a reasonable time, but do not necessarily have to regarding the common good [10]. To provide the optimal performance regarding a system's objective, for example fast data delivery in the network or low power consumption on the UAVs for a long-term service, operators of the aerial communication support system have to consider a plethora or parameters and it must also be highly flexible to allow for the required adaptions. Furthermore, the communication performance of inter-cluster links is not only dependent on the disaster scenario itself, but even more so on the available UAVs and their flight properties. With a possibly very heterogeneous set of available commodity UAVs with different ranges, velocities, flight times, and more, taking only a few parameters into account for an optimal solution is very complex, and the required re-evaluation after changing the target communication performance for example, places additional burdens for operating personnel.

We therefore automate the process of finding system settings providing the desired communication performance. This relieves the operating personnel but also allows to optimize the process in the first place based on chosen requirements. An analysis of multiple requirements on the communication performance and the data ferry links revealed three general approaches to optimize the settings of such a system. These approaches are namely *link-energy-efficiency*, *ferry-time-efficiency*, and *message-energy-efficiency* which will be discussed in the following. From a wide range of available system settings, the UAV's velocity v moving on the link between clusters and the time period t_d it hovers over an cluster while distributing and collecting messages are most influential on the communication performance. The maximum possible velocity v_{max} is defined by the multicopter UAV and restricts v such that $0 < v \leq v_{max}$. And furthermore, the operator may restrict t_d such that $t_{d,min} \leq t_d \leq t_{d,max}$ with minimum and maximum boundaries for the distribution time.

A. Link-Energy-Efficiency

The *link-energy-efficiency* optimization maximizes the usage of a UAV's battery power while also maximizing the number of round trips to prolong the time a UAV can provide the communication support before requiring to be reloaded or exchanged. A round trip for a UAV on a link is defined as the way from one network cluster to the other and back. We also define one of the network clusters as handover position, thus, as the cluster where the UAV exchange happens, which is the one cluster that is closer to the recharging station. A full round trip starts and also ends at this cluster. Therefore, the distance traveled for one round trip d_{RT} is equal to two times the distance $d_{cluster}$ between the clusters, and furthermore, the time required for one round trip depends on the distance, the link velocity v, and the distribution time t_{dist}, such that

$$t_{RT}(v, t_{dist}) = 2 * \frac{d_{cluster}}{v} + 2 * t_{dist} = \frac{d_{RT}}{v} + 2 * t_d. \quad (8)$$

Similar, the energy that is required for one round trip can be calculated as

$$E_{RT}(v, t_{dist}) = \frac{d_{RT}}{v} * E(v) + 2 * t_{dist} * E_{hover} \quad (9)$$

where $E(v)$ is the energy that is required for flying with velocity v and E_{hover} the energy for hovering. The energy consumption is calculated using the propulsion energy model as introduced in Section III. In combination with the overall energy available in the battery, we can calculate the number of full round trips that are achievable by the UAV as

$$n_{RT}(v, t_{dist}) = \left\lfloor \frac{E_{usage}}{E_{RT}(v, t_{dist})} \right\rfloor \quad (10)$$

where E_{usage} is the amount of energy that is available for the flight. For safety reasons, we define a battery threshold e_{thresh} that, when reached, triggers an immediate return to the recharging station, to prevent a loss of the UAV by battery failure. Furthermore, the usable energy is also reduced by the energy E_{hop} which is required to reach the handover position from the recharging station.

$$E_{usage} = E_{battery} * (1 - e_{thresh}) - E_{hop}. \quad (11)$$

Therefore, the *link-energy-efficiency* $LEE(v, t_{dist}) \in [0, 1]$ estimates the amount of used battery power:

$$LEE(v, t_{dist}) = \frac{E_{RT}(v, t_{dist}) * n_{RT}(v, t_{dist})}{E_{usage}}. \quad (12)$$

B. Ferry-Time-Efficiency

The optimization function for *ferry-time-efficiency* is used to minimize the delivery delay of inter-cluster communication. The worst-case scenario for message transportation between two clusters is that a message is generated shortly after the UAV has departed. In that case, the message will remain in the cluster until the UAV returns and just then transports it over to the other cluster. Using the worst possibility to describe the transport time of the data ferry has the advantage of being applicable for all messages at once, not just a subset. The *ferry-time-efficiency* $FTE(v, t_{dist})$ is, therefore, independent of the energy consumption and can be described as

$$FTE(v, t_{dist}) = 3 * \frac{d_{cluster}}{v} + 2 * t_{dist} \quad (13)$$

which results in an estimation for an overall transport duration.

C. Message-Energy-Efficiency

With the *message-energy-efficiency* function, system settings are adapted to minimize the amount of energy that the transportation of each message over the data ferry link consumes, by increasing the amount of messages transported by the UAV but also decreasing the energy that is used for the movement itself. Although messages might be stored longer in the UAV's memory, we only take messages that are new and are not known on the destination network cluster into consideration for the calculation. Furthermore, the rate of messages that are created within a certain time frame r_{msg} must be known or anticipated a priori, e.g., by monitoring the DTN-MANET beforehand, to be able to calculate the optimized system settings. As this rate is an average value, we do not use the worst-case estimation for the transport time, but the average round trip time as shown in Equation 8. The *message-energy-efficiency* function

$$MEE(v, t_{dist}) = \frac{E_{RT}(v, t_{dist})}{t_{RT} * r_{msg}} \quad (14)$$

calculates the average energy consumption per transported messages.

D. Additional Side Conditions

In some specific scenarios, optimizations will result in system settings with which the UAV cannot fly even one full round trip, mostly when $d_{cluster}$ is large in comparison to the UAV flight range. We therefore define the side condition (1) $n_{RT}(v, t_d) \geq 1$ (cf. Eq. 10), so that the given settings allow at least one round trip. If this cannot hold at any setting, the available UAVs are not suitable for the respective scenario and we have to re-evaluate the situation. Error handling if this applies, however, is out of the scope of this paper.

Furthermore, an optional parameter t_{RT-max} is included, which resembles an upper limit for the overall round trip duration. If the operator sets it, for example, to the lifetime value of messages in the DTN-MANET, it guarantees that all messages are distributed between the two clusters within their lifetime. When activated, side condition (2) $t_{RT}(v, t_d) \leq t_{RT-max}$ (cf. Eq. 8) must hold for all optimization functions.

E. Weighted Combination Optimization Model

Apart from prioritizing distribution time, UAV service time, or energy consumption per transported message alone, respectively, the system operator could emphasize multiple objectives, such as quick dissemination but also moderate transport energy. For this case, we use weights for each optimization function such that $w_{LEE} + w_{FTE} + w_{MEE} = 1$. Naturally, setting one of these weights to 1 is the same as using the respective function alone. The operator can state the

preferences for each objective by the weights and an overall solution

$$F_{comb}(v, t_{dist}) = w_{LEE} * LEE(v, t_d) + w_{FTE} * FTE(v, t_{dist}) + w_{MEE} * MEE(v, t_{dist}) \quad (15)$$

can be calculated as the combination of the weighted and normalized functions.

The optimization model uses the function to calculate the combined score $F_{comb}(v, t_{dist}) \in [0, 1]$ for a pair (v, t_{dist}). To find the optimal values for v and t_{dist}, we use a numerical approach by calculating F_{comb} for each pair within the given boundaries $t_{dist,min} \leq t_{dist} \leq t_{dist,max}$ and $v_{min} \leq v \leq v_{max}$. Values for v and t_{dist} are incremented by $\Delta v = 0.5 \frac{m}{s}$ and $\Delta t = 1\,s$, respectively. The increments, however, can be changed if necessary.

V. Simulation Results

The optimization model and the energy consumption model (cf. Section III) were both implemented as additions to the simulation platform for Unmanned Aerial Systems, which was described in [13]. Before a UAV is dispatched to a specific data ferry link, the optimization model calculates the best link velocity v and message dissemination time t_{dist} based on the energy model and battery constraints of the respective UAV and the optimization weights given by the operator. Resulting parameters are used to program the UAV, which then takes off and then transport data between the network clusters of the specific link. The simulation environment was specifically chosen to evaluate the influence of the different functions and also the weighted combination of them. We defined a single link between two network clusters, one located around a hospital and one at a school, with a distance of $d_{cluster} = 2$km in an inner-city environment in Darmstadt, Germany. The link is constantly served by one UAV, while a second UAV is ready to replace the first when necessary. The recharging station is placed in the courtyard of the local fire brigade, around 350m from the network cluster at the hospital, from where a UAV system could be operated reasonably. Each simulation was performed with 100 DTN-MANET nodes that moved around a 100 m radius around the hospital and the school, respectively. Nodes were placed randomly on the map and used a pedestrian movement model with map data from Open Street Map[3]. The target location the nodes will gather around is also chosen randomly, resulting in similar but unevenly split DTN-MANET clusters as network clusters. All simulations were repeated with ten different random seeds and simulated a duration of 5 hours. Messages were generated a rate of approximately 10 per minute, which was used to define r_{msg}, each of them from a randomly chosen node with all nodes as targeted recipient (broadcast). The message lifetime (time-to-live, TTL) was set to 10 and 20 minutes, respectively, and the optional parameter t_{TR-max} used for the guarantee of timely message delivery in side condition (2) was set to the same value as the applied TTL. The battery threshold e_{thresh} was set to 15%, which is sufficient to return to the base in this scenario.

[3]Open Street Map, www.openstreetmap.org (accessed 16.05.2019)

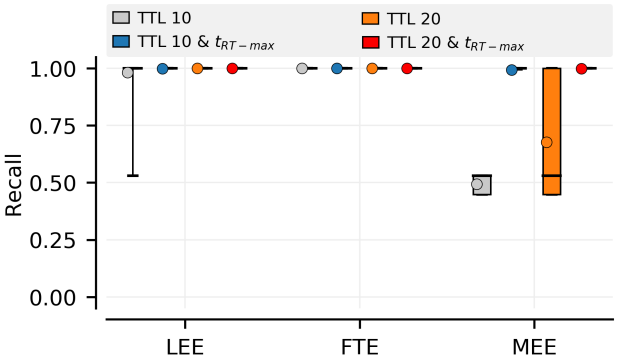

Fig. 2: Message recall (percentage of reached nodes) with 10 and 20 minutes message lifetime, respectively. Omitting side condition 2 (t_{TR-max}) has significant impact for MEE, because messages expire during transport, and thus, do not reach the other cluster.

Figure 2 shows the recall, i.e., the percentage of nodes that eventually received one message, for each optimization, respectively. Whiskers indicate the 2.5th and 97.5th percentiles, colored boxes the 25th and 75th percentiles, bold dashes the median, and colored circles the mean values, respectively. For example, optimizing for link efficiency (LEE) with a 10 minute TTL and side condition (2), all messages are distributed to all nodes. Removing side condition (2), however, leads to a degradation of message dissemination. As indicated by the whisker, around 25% of messages do not reach the other side of the link in that case.

Thus, using or omitting the side condition t_{TR-max} has significant influence on message dissemination, especially when optimizing for minimal transport energy (MEE). When omitted, MEE chooses the distribution time t_d high and the flight velocity $v = v_{min}$, and thus, message transport takes too long to be successful. In our simulations with 10 minutes TTL, this resulted in not a single successfully transported messages over the link, as indicated by a mean recall of 50%. The shown deviation indicates the unevenly split network clusters, as described above. Even when using a 20 minutes TTL without the side condition, only 25% of messages reach the other side of the data ferry link. The ferry time optimization (FTE) aims for fast dissemination, thus, t_d is always chosen minimal and v is always chosen maximal. Therefore, the side condition does not have any effect here.

Especially for the application in disaster scenarios, we think a complete message dissemination among the network clusters to have top priority. As a conclusion, we will always use the side condition t_{TR-max} in the further course of the evaluation.

Figure 3 shows the delivery delay of messages for 10 and 20 minutes message lifetime, respectively. The lowest delay is reached with the ferry time optimization (FTE) due to picking minimal t_d and maximal v. Thus, we can already deduce that

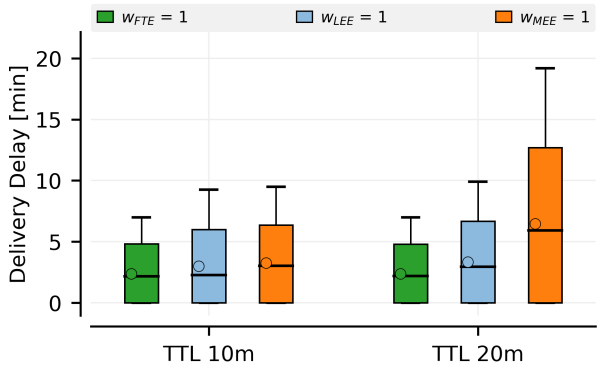

Fig. 3: FTE optimization is independent of applied TTLs, as the fastest parameters are always chosen. In contrast, MEE minimizes transport energy by fully utilizing the TTL.

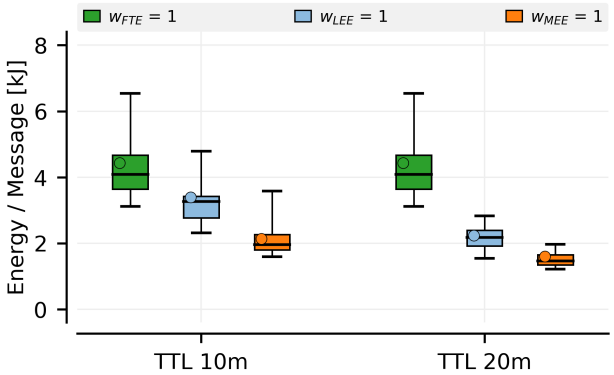

Fig. 4: Optimizing for message transport energy efficiency utilizing MEE more than halves the energy expense in comparison to the optimization for fastest delivery using FTE.

the FTE optimizer returns the parameter settings as expected. With 10 minutes message lifetime, the optimizers for link (LEE) and message energy (MEE), respectively, perform similar in delivery delay. For 20 minutes TTL, however, MEE uses the available time more fully to wait longer and transport more messages in one link traversal, resulting in significantly increased delivery delays in this case, whereas LEE only slightly increases.

The expended energy to transport messages is depicted in Figure 4, showcasing the influence of MEE to minimize message transport energy. In comparison to the fastest delivery (FTE), energy expense can be more than halved, especially for 20 minutes TTL. The difference between MEE and LEE, however, is smaller as expected, presumably due to the similar goal of energy minimization. Link energy optimization (LEE) uses short dissemination times and the most efficient velocity (cf. Fig. 4) to maximize both the number of possible round trips and battery utilization. The measured battery level when returning to the base station after the exchange UAV has arrived is 14.5% on average, showing that available energy is fully utilized for link flights. The message energy optimizer (MEE), on the contrary, picks slow speeds and long dissemination times to minimize the transport energy. Interestingly, this results in less ferry exchanges using MEE than LEE required for the continuous service during the simulation time, because LEE results in higher velocities, and thus, higher power consumption.

In case of combining different functions, the resulting parameter settings cannot always be intuitively anticipated because some features like the number of possible round trips are not steady. It is therefore necessary to assess the influence of different weight combinations for the operator to find the matching system settings. Furthermore, each scenario is different, and thus, needs individual examination. The resulting design space of optimization functions and parameter combinations is highly complex. To demonstrate the possibility of finding suitable weights, Figure 5 shows delivery delay and transport energy per message when combining the ferry time optimizer with the message energy optimizer. The weights $w_{FTE} = 1$ are shifted towards $w_{MEE} = 1$ with a difference of $\Delta w = 0.1$ in each step. The weight for the link energy optimizer w_{LEE} is 0 in all these cases. It can be seen that the delivery delay is increasing when more weight is put on energy efficiency than on delivery delay. The transport energy, in contrast, decreases at the same time. If the operator searches for system settings that are a trade-off between transport energy and delivery delay, this helps picking the weights, e.g., as $w_{FTE} = 0.6$ and $w_{MEE} = 0.4$ to reduce energy consumption by a factor of two while still delivering most of the messages within 10 minutes.

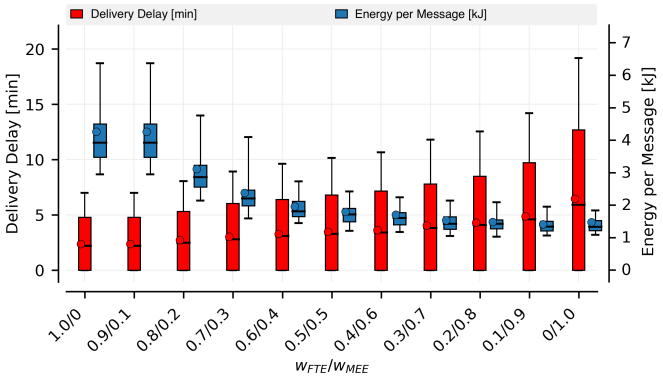

Fig. 5: Delivery delay and transport energy per message. Weight combinations were shifted in ten steps of $\Delta w = 0.1$ from $w_{FTE} = 1$ towards $w_{MEE} = 1$.

VI. Conclusion

In this paper we presented three different approaches optimizing inter-cluster flights of data ferry UAVs as communication support in highly intermittent DTN-MANETs. A configurable optimization model seamlessly combines the different optimization functions in case that multiple objectives are pursued by the support system. Furthermore, we designed a velocity-based energy consumption model for multicopter UAVs based on a real-world counterpart, that is required by

the optimization model for a realistic estimation of energy consumption. Both models were implemented and simulated in an existing simulation framework for Unmanned Aerial Systems [13].

Evidently, more complex scenarios like communication between multiple network clusters or highly varying network loads will further increase the complexity of the system and might require different optimization functions. Furthermore, simulations were conducted with the flight properties of the presented real-world multicopter UAV in an inner-city scenario. Although the optimization model is applicable for scenarios of different sizes, it may not be suitable for fixed-wing UAVs due to their inability to hover and an inherently different movement from that of multicopter UAVs. Besides these two examples, there are still many open issues regarding the optimization of complex data ferry applications. However, the presented configurable optimization model not only allows for extensive system assessments, but also provides the ability to find the most suitable system settings based on available UAVs and their flight properties, cluster locations and distances, as well as requirements on the support system. It is therefore a powerful tool for operators of aerial communication support systems in post-disaster scenarios.

ACKNOWLEDGMENT

This work has been co-funded by the LOEWE initiative (Hessen, Germany) within the *Nature 4.0 – Sensing Biodiversity* project and the German Research Foundation (DFG) in the Collaborative Research Center (SFB) 1053 *MAKI – Multi-Mechanisms Adaption for the Future Internet*.

REFERENCES

[1] M. Ahmed, S. Krishnamurthy, R. Katz, and S. Dao, "Trajectory control of mobile gateways for range extension in ad hoc networks," *Computer Networks*, vol. 39, no. 6, pp. 809–825, 2002.

[2] F. Álvarez, L. Almon, P. Lieser, T. Meuser, Y. Dylla, B. Richerzhagen, M. Hollick, and R. Steinmetz, "Conducting a Large-scale Field Test of a Smartphone-based Communication Network for Emergency Response," in *Proceedings of the 13th Workshop on Challenged Networks*. ACM, 2018, pp. 3–10.

[3] K. Anazawa, P. Li, T. Miyazaki, and S. Guo, "Trajectory and data planning for mobile relay to enable efficient internet access after disasters," in *2015 IEEE Global Communications Conference (GLOBECOM)*. IEEE, 2015, pp. 1–6.

[4] A. Blum, P. Chalasani, D. Coppersmith, B. Pulleyblank, P. Raghavan, and M. Sudan, "On the minimum latency problem," 1994.

[5] E. Bonomi and J.-L. Lutton, "The N-city travelling salesman problem: Statistical mechanics and the Metropolis algorithm," *SIAM review*, vol. 26, no. 4, pp. 551–568, 1984.

[6] J. B. Brandt, R. W. Deters, G. K. Ananda Krishnan, and M. S. Selig. UIUC Propeller Database. University of Illinois at Urbana-Champaign. [Online]. Available: http://m-selig.ae.illinois.edu/props/propDB.html

[7] Z. Han, A. L. Swindlehurst, and K. R. Liu, "Optimization of manet connectivity via smart deployment/movement of unmanned air vehicles," *IEEE Transactions on Vehicular Technology*, vol. 58, no. 7, pp. 3533–3546, 2009.

[8] S. Hayat, E. Yanmaz, and C. Bettstetter, "Experimental analysis of multipoint-to-point UAV communications with IEEE 802.11n and 802.11ac," in *Personal, Indoor, and Mobile Radio Communications (PIMRC), 2015 IEEE 26th Annual International Symposium on*. IEEE, 2015, pp. 1991–1996.

[9] A. Khelil, P. J. Marrón, C. Becker, and K. Rothermel, "Hypergossiping: A generalized broadcast strategy for mobile ad hoc networks," *Ad Hoc Networks*, vol. 5, no. 5, pp. 531–546, 2007.

[10] P. Lieser, F. Alvarez, P. Gardner-Stephen, M. Hollick, and D. Boehnstedt, "Architecture for Responsive Emergency Communications Networks," in *Global Humanitarian Technology Conference (GHTC). IEEE*, 2017.

[11] P. Lieser, N. Richerzhagen, T. Feuerbach, T. Meuser, B. Rocherzhagen, and R. Steinmetz, "Collaborative Decentralized Resource Reservation for Emergency Communication Networks," in *43rd IEEE Conference on Local Computer Networks (LCN)*, 2018.

[12] P. Lieser, N. Richerzhagen, S. Luser, B. Richerzhagen, and R. Steinmetz, "Understanding the Impact of Message Prioritization in Post-Disaster Ad Hoc Networks," in *Proceedings of the 4th International Conference on Networked Systems (NetSys)*. ACM, 2019.

[13] P. Lieser, J. Zobel, B. Richerzhagen, and R. Steinmetz, "Simulation Platform for Unmanned Aerial Systems in Emergency Ad Hoc Networks," *Proceedings of the 16th International Conference on Information Systems for Crisis Response and Management (ISCRAM)*, 2019.

[14] A. Lindgren, A. Doria, and O. Schelen, "Probabilistic routing in intermittently connected networks," in *Service assurance with partial and intermittent resources*. Springer, 2004, pp. 239–254.

[15] A. Mori, H. Okada, K. Kobayashi, M. Katayama, and K. Mase, "Construction of a node-combined wireless network for large-scale disasters," in *Consumer Communications and Networking Conference (CCNC), 2015 12th Annual IEEE*. IEEE, 2015, pp. 219–224.

[16] M. Mozaffari, W. Saad, M. Bennis, and M. Debbah, "Mobile Unmanned Aerial Vehicles (UAVs) for Energy-efficient Internet of Things Communications," *IEEE Transactions on Wireless Communications*, vol. 16, no. 11, pp. 7574–7589, 2017.

[17] D. Nain, N. Petigara, and H. Balakrishnan, "Integrated routing and storage for messaging applications in mobile ad hoc networks," *Mobile Networks and Applications*, vol. 9, no. 6, pp. 595–604, 2004.

[18] J. A. Paredes, C. Saito, M. Abarca, and F. Cuellar, "Study of Effects of High-altitude Environments on Multicopter and Fixed-wing UAVs' Energy Consumption and Flight Time," in *2017 13th IEEE Conference on Automation Science and Engineering (CASE)*. IEEE, 2017, pp. 1645–1650.

[19] B. Pearre and T. X. Brown, "Model-free Trajectory Optimisation for Unmanned Aircraft Serving as Data Ferries for Widespread Sensors," *Remote Sensing*, vol. 4, no. 10, pp. 2971–3005, 2012.

[20] Prof. Z. S. Spakovszky. Thermodynamics and Propulsion: Performance of Propellers. Massachusetts Institute of Technology (MIT). [Online]. Available: http://web.mit.edu/16.unified/www/SPRING/thermodynamics/notes/node86.html

[21] T. Spyropoulos, K. Psounis, and C. S. Raghavendra, "Spray and wait: an efficient routing scheme for intermittently connected mobile networks," in *Proceedings of the 2005 ACM SIGCOMM workshop on Delay-tolerant networking*. ACM, 2005, pp. 252–259.

[22] H. Toya and M. Skidmore, "Cellular telephones and natural disaster vulnerability," *Sustainability*, vol. 10, no. 9, p. 2970, 2018.

[23] N. Uchida, N. Kawamura, K. Takahata, Y. Shibata, and N. Shiratori, "Proposal of data triage methods for disaster information network system based on delay tolerant networking," in *Broadband and Wireless Computing, Communication and Applications (BWCCA), 2013 Eighth International Conference on*. IEEE, 2013, pp. 15–21.

[24] A. Vahdat, D. Becker *et al.*, "Epidemic routing for partially connected ad hoc networks," 2000.

[25] J. Whitbeck and V. Conan, "HYMAD: Hybrid DTN-MANET routing for dense and highly dynamic wireless networks," *Computer communications*, vol. 33, no. 13, pp. 1483–1492, 2010.

[26] Y. Zeng and R. Zhang, "Energy-efficient UAV communication with trajectory optimization," *IEEE Transactions on Wireless Communications*, vol. 16, no. 6, pp. 3747–3760, 2017.

[27] Y. Zeng, R. Zhang, and T. J. Lim, "Throughput maximization for UAV-enabled mobile relaying systems," *IEEE Transactions on Communications*, vol. 64, no. 12, pp. 4983–4996, 2016.

[28] W. Zhao, M. Ammar, and E. Zegura, "A message ferrying approach for data delivery in sparse mobile ad hoc networks," in *Proceedings of the 5th ACM international symposium on Mobile ad hoc networking and computing*. ACM, 2004, pp. 187–198.

[29] K. Zhou and T. M. Lok, "Optimal power allocation for relayed transmission through a mobile relay node," in *2010 IEEE 71st Vehicular Technology Conference*. IEEE, 2010, pp. 1–5.

[30] C. D. Zorrilla, "The view from Puerto Rico – Hurricane Maria and its aftermath," *New England Journal of Medicine*, vol. 377, no. 19, pp. 1801–1803, 2017.